

Available online at
ScienceDirect
 www.sciencedirect.com

Elsevier Masson France
EM|consulte
 www.em-consulte.com



Original Article

Tumor radiomics signature for artificial neural network-assisted detection of neck metastasis in patient with tongue cancer

Yi-Wei Zhong^{a,1}, Yin Jiang^{b,c,1}, Shuang Dong^a, Wen-Jie Wu^{a,*}, Ling-Xiao Wang^{d,e}, Jie Zhang^a, Ming-Wei Huang^a

^a Department of Oral and Maxillofacial Surgery, Peking University School and Hospital of Stomatology, Beijing, PR China

^b Department of Physics, Beihang University, Beijing, PR China

^c Beijing Advanced Innovation Center for Big Data-based Precision Medicine, Beihang University, Beijing, PR China

^d Department of Physics, Tsinghua University, Beijing, PR China

^e Frankfurt Institute for Advanced Studies, Frankfurt am Main, Germany

ARTICLE INFO

Article History:

Available online 4 August 2021

Keywords:

Tongue
 Squamous cell carcinoma
 Lymph node
 Computed tomography
 Artificial intelligence

ABSTRACT

Background and purpose: To determine the neck management of tongue cancer, this study attempted to construct an artificial neural network (ANN)-assisted model based on computed tomography (CT) radiomics of primary tumors to predict neck lymph node (LN) status in patients with tongue squamous cell carcinoma (SCC).

Materials and methods: Three hundred thirteen patients with tongue SCC were retrospectively included and randomly divided into training (60%), validation (20%) and internally independent test (20%) sets. In total, 1673 feature values were extracted after the semiautomatic segmentation of primary tumors and set as input layers of a classical 3-layer ANN incorporated with or without clinical LN (cN) status after dimension reduction. The receiver operating characteristic (ROC) curve, accuracy (ACC), sensitivity (SEN), specificity (SPE), area under curve (AUC) and Net Reclassification Index (NRI), were used to evaluate and compare the models. **Results:** Four models with different settings were constructed. The ACC, SEN, SPE and AUC reached 84.1%, 93.1%, 76.5% and 0.943 (95% confidence interval: 0.891–0.996, $p < .001$), respectively, in the test set. The NRI of models compared with radiologists reached 40% ($p < .001$). The occult nodal metastasis rate was reduced from 30.9% to a minimum of 12.7% in the T1–2 group.

Conclusion: ANN-based models that incorporated CT radiomics of primary tumors with traditional LN evaluation were constructed and validated to more precisely predict neck LN metastasis in patients with tongue SCC than with naked eyes, especially in early-stage cancer.

© 2021 Elsevier Masson SAS. All rights reserved.

Introduction

The neck lymph node (LN) status significantly affects the survival rate and determines the surgery protocol of oral cancer^{1,2}; especially in tongue cancer, a subsite occupying approximately 1/3 of the oral cancer, with 20–40% of the patients suffering from occult neck metastasis.³ Accurate preoperative detection of these occult nodal metastasis is necessary.

Multiple radiological methods are available for the detection of LN metastasis of head and neck cancer.^{4,5} Among which, computed tomography (CT), a noninvasive, time-saving and economic modality, is most widely used to provide information for preoperative nodal

staging based on morphological changes,^{3,6} with an accuracy that depends on the experience of the radiologists while with naked eyes and has been improved by assisted tools.

However, most of the tools were at the nodal levels,^{7–9} ignoring the radiologically invisible nodal metastasis which clinicians more attended to. And those at the patient levels^{10,11} showed potential of the nodal metastasis predictive ability from primary tumors while with demerits like postoperative assessment, small and non-homogeneous dataset, relatively low accuracy, and uncommon instruments which made them less convincing and accessible for clinical application. What's more, the proportion of early stage where controversy on whether neck dissection should be performed existed, is limited.¹⁰ Thus, improvement is needed.

Radiomics is a method that clinicians and radiologists use to convert medical imaging into high-dimensional quantitative data for research on clinical decision-making support.¹² Theoretically, radiomics can noninvasively facilitate quantifying tumor heterogeneity at

* Corresponding author at: No. 22 Zhongguancun South Avenue, Department of Oral and Maxillofacial Surgery, Peking University School and Hospital of Stomatology, Beijing, 100081, China.

E-mail address: wenjiewu@bjmu.edu.cn (W.-J. Wu).

¹ Yi-Wei Zhong, M.M., and Yin Jiang, Ph.D. contributed equally to this work.

the morphological, genic and even molecular levels based an automated data characterization algorithm to provide information concerning the staging, diagnosis, prognosis, and prediction of treatment responses.^{13,14} Many studies have successfully applied tumor radiomics feature analysis to predict the node status of cervical cancer, bladder cancer, colorectal cancer, etc., and achieved satisfactory accuracy.^{15–18} Accordingly, we assume that the CT radiomics of tongue cancer may have high value in predicting neck LN status.

While facing massive datasets, researchers often turn to artificial neural network (ANN) for the strength in fields involving high-dimensional data with nonlinear relationships.¹⁹ Therefore, in this study, we will show our attempt to construct and validate ANN models for the prediction of neck LN metastasis in tongue cancer based on CT radiomics and related clinical factors, and assess the application on early stage tumors, especially on the occult metastasis.

Material and methods

Study design

This diagnostic study was approved by the ethics committee and conducted under the guidance of international ethical standards (IRB number: PKUSSIRB-202059160). Patients with tongue cancer between January 2013 and December 2018 were enrolled retrospectively according to the following inclusion criteria: (a) underwent primary tumor resection and neck dissection (ND); (b) histologically diagnosed with squamous cell carcinoma (SCC) and examined for cervical LN enlargement; (c) available contrast-enhanced computed tomography (CECT) data for the head and neck region performed fewer than 20 days before surgery; and (d) detailed clinical information. The exclusion criteria were as follows: (a) previous tumors; (b) preoperative chemotherapy or radiotherapy; (c) distant metastasis before surgery; (d) no visible tumor lesion on CT scans; (e) radiological interference from artifacts. The recruitment pathway is shown in Fig. 1.

The surgical protocol was in accordance with the National Comprehensive Cancer Network (NCCN) guidelines. Positive clinical LN (cN) status was defined as at least one node with rounded contour, cystic or necrotic change, enlargement, or ill-defined margins detected on CT according to the American Joint Committee on Cancer (AJCC) Cancer Staging Manual, eighth edition. The pathological LN (pN) status and degree of differentiation were determined by histopathological examination, and the pN status was regarded as the gold standard.

CT imaging protocol

CECT scanning of the head and neck with a 512×512 matrix, $0.4 \times 0.4 \times 0.75$ mm³ voxel size, tube voltage of 120 kV, and tube current of 225–300 mA was performed on all patients 60 seconds after administration of intravenous iopamidol (1.2 mL/kg, 2 mL/s, 370 mg I/mL, Bracco) using a GE Optima CT680 scanner. The images were exported in Digital Imaging and Communications in Medicine (DICOM) format for image feature extraction.

ROI segmentation

Semiautomatic tumor segmentation of the CECT dataset was performed independently by a radiologist with 8 years' experience in head neck imaging and was blinded to the clinic-pathological information of patients, using a free and open source software (3D Slicer, version 4.10.1; available at <http://slicer.org/>). First, the tumor lesion region and surrounding tissue region were roughly delineated manually. Next, the Fast GrowCut algorithm²⁰ implemented in 3D Slicer contoured the tumor lesion region automatically and transformed it into the region of interest (ROI). Third, the radiologists scrutinized the ROI and repeated the previous steps until adjacent hard tissue and air were removed from the ROI. Finally, the ROI and the original CT dataset were exported and imported to the Imaging Biomarker Explorer (IBEX),²¹ an open source software based on MATLAB 2014b (MathWorks). Besides, another radiologist with 4 years' experience in head neck imaging, performed ROI drawing of 60 random chosen patients independently to evaluate the inter-observer variability of model prediction.

Feature extraction and dimension reduction

Features and relevant parameters were extracted from the ROI of each patient through IBEX without preprocessing, and missing values were deleted. The categories and parameters of the features are listed in **Supplementary 1**. Then, principal component analysis (PCA), carried out in MATLAB 2018b (MathWorks), was used to reduce the dimension of the features without destroying the derivation of the raw data and generate combined feature groups.

Construction and validation of the ANN model

A classical 3-layer design was adopted for the architecture of the ANNs in MATLAB 2018b. The combined feature groups with or without the cN status were added as nodes in the input layer. Certain hidden layers and one single output layer were used to process the data

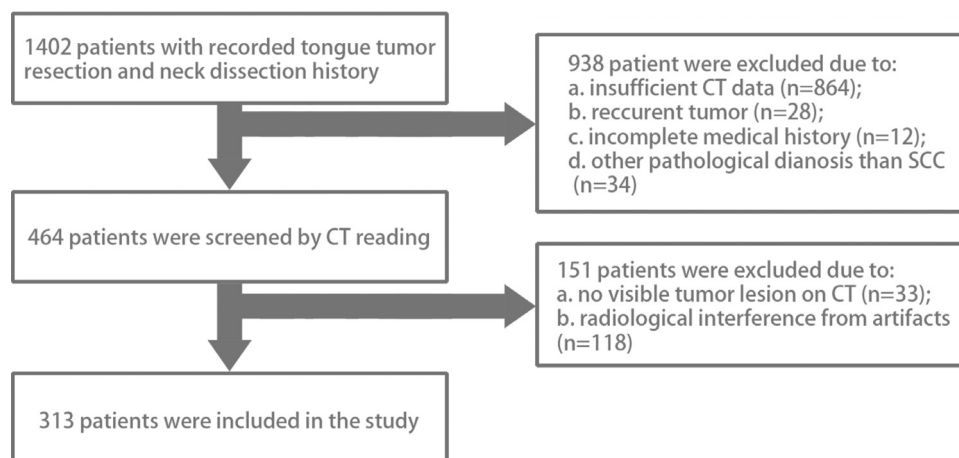


Fig. 1. The recruitment pathway.

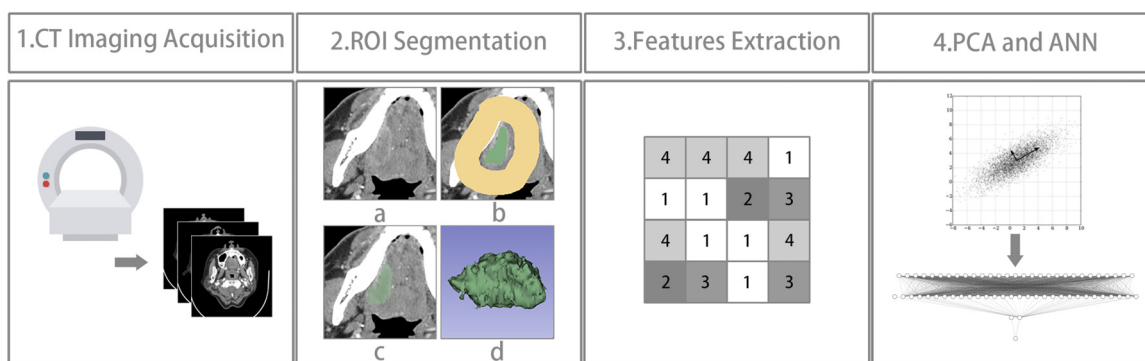


Fig. 2. The workflow diagram of the model architecture. First, the CT data of the patients were acquired. Second, semiautomatic segmentation of the ROI by rough manual delineation and the Fast GrowCut algorithm. Third, the radiomics features were extracted. Fourth, dimension reduction by PCA (the diagram was derived from that in en.m.wikipedia.org/wiki/Principle_component_analysis) and modeling by the ANN were performed.

and produce the outcome value under different weights. Bias was added to avoid overfitting during the process. The patients were randomly divided into training (187, 80%), validation (63, 20%) and internally independent test (63, 20%) sets. The patient data with negative clinical LN status (cN0) and early-stage cancer (T1-2cN0) underwent more rounds of training by an ensemble learning algorithm. The outcome values were transformed into integers by the round function. Then, the training process by the Levenberg-Marquardt algorithm kept updating the weights and parameters in the ANNs to ensure that the outputs of the network were close to the gold standard pN for each case.

Statistical analysis

The intra-class correlation coefficient (ICC) was calculated to evaluate the inter-observer variability of all models prediction result with SPSS 26.0, and models with ICC value no less than 0.75 were regarded as highly reproducible. The occult nodal metastasis rate in group T1-2, Net Reclassification Index (NRI) compared with cN,²² area under the curve (AUC), sensitivity (SEN), specificity (SPE), accuracy (ACC) and receiver operating characteristic (ROC) curve of the models and prediction from radiologists were determined for different groups with MATLAB 2018b. The level of statistical significance of *p* value were defined as .05. The whole workflow is displayed in Fig. 2.

Table 1
The clinical baseline information of patients included.

pN	Positive <i>n</i> = 143	Negative <i>n</i> = 170	<i>p</i>
Age			.910
Mean±SD	55.15±12.89	54.99±12.03	
Median	55.00	55.00	
Gender			.164
Female	63	61	
Male	80	109	
T Classification			.008
T1	28 (19.2%)	59 (34.7%)	
T2	74 (51.7%)	82 (48.2%)	
T3	12 (8.4%)	6 (3.5%)	
T4	29 (20.3%)	23 (13.5%)	
Max Size			<.001
Mean±SD	3.16±1.22	2.63±1.05	
Median	3.00	2.50	
Histological Grade			.158
I	25	68	
II	109	97	
III	9	5	

pN: pathological lymph node status, SD: standard deviation.

Results

Out of a total of 1402 patients from January 2013 to December 2018, 313 patients who met the inclusion criteria were included in this study cohort. The clinical characteristics of these 313 patients are summarized in Table 1. After the 94 values listed in Supplementary 2 were excluded for missing data, 1673 values of 141 features in 10 categories were extracted and included.

The completeness rate *q* of the original features was set to 0.95 and 0.99 for data reduction. As a result, 28 and 83 groups of combined features were generated, respectively. The features ranked by PCA were divided into positive relative and negative relative groups and are listed in Supplementary 3-6. In total, 4 ANN models named after the input items and *q* value were constructed, which included a model with radiomics incorporated with cN and a *q* of 0.95 (cNRAD95), a model with radiomics incorporated with cN and a *q* of 0.99 (cNRAD99), a model with radiomics and a *q* of 0.95 (RAD95) and a model with radiomics and a *q* of 0.99 (RAD99). According to the input items, 28, 29, 83, and 84 nodes were set in both the input layer and the hidden layer in the RAD95, cNRAD95, RAD99, and cNRAD99 models, respectively. The code of the ANNs was uploaded in GitHub (<https://github.com/zyw-kq/Models>).

Table 2
Performance of models.

Group	Model	Accuracy	Sensitivity	Specificity	AUC (95%CI)*
All	cN	73.6%	53.8%	90.6%	-
	cNRAD95	86.9%	83.9%	90.0%	0.934 (0.908-0.961)
	cNRAD99	87.6%	84.6%	90.6%	0.936 (0.909-0.964)
	RAD95	75.5%	68.5%	81.8%	0.827 (0.782-0.873)
cN0	RAD99	84.1%	81.8%	86.5%	0.919 (0.890-0.949)
	cNRAD95	85.5%	65.2%	94.2%	0.912 (0.870-0.954)
	cNRAD99	87.7%	68.2%	96.1%	0.931 (0.893-0.968)
	RAD95	77.7%	65.2%	83.1%	0.816 (0.754-0.878)
T1-2	RAD99	85.5%	83.3%	86.4%	0.926 (0.891-0.960)
	cN	71.6%	43.1%	92.2%	-
	cNRAD95	88.1%	81.4%	92.9%	0.937 (0.906-0.968)
	cNRAD99	86.8%	81.4%	90.8%	0.932 (0.900-0.963)
T1-2cN0	RAD95	76.5%	62.7%	86.5%	0.826 (0.773-0.880)
	RAD99	84.0%	78.4%	87.9%	0.919 (0.887-0.952)
	cNRAD95	86.7%	67.2%	95.4%	0.920 (0.876-0.964)
	cNRAD99	86.7%	67.2%	95.4%	0.930 (0.889-0.970)
Test set	RAD95	79.8%	63.8%	86.9%	0.837 (0.773-0.902)
	RAD99	86.2%	82.8%	87.7%	0.933 (0.899-0.967)
	cNRAD95	82.5%	64.3%	97.1%	0.946 (0.895-0.997)
	cNRAD99	84.1%	93.1%	76.5%	0.943 (0.891-0.996)
	RAD95	85.7%	74.1%	94.4%	0.899 (0.815-0.983)
	RAD99	85.7%	82.1%	88.6%	0.917 (0.850-0.984)

AUC: area under curve; CI: confidence intervals.

* The *p* values were all less than .001

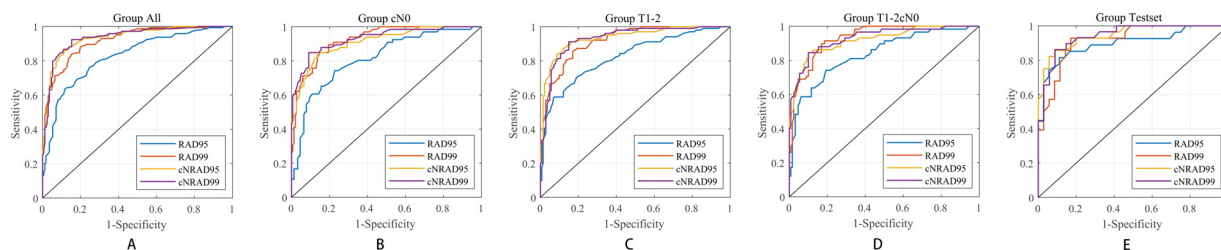


Fig. 3. The ROC curves of models are shown in group All (A), cN0 (B), T1-2 (C), T1-2cN0 (D) and Test set (E) respectively. The ROC curves show good performance of the models in the test set group and in the group of all patients. The RAD95 model is the worst-performing model, while the other three models perform well in certain parts of the curves in different groups, which implies different indications for models of different stages.

All the ICC value of the models were no less than 0.75. The AUC with 95% confidence intervals (95%CI), SEN, SPE and ACC of the cN, RAD95, RAD99, cNRAD95 and cNRAD99 models for predicting pN and the performance of all the models on the patient groups of the test set, cN0, early primary tumor stage (T1-2) and T1-2cN0 are listed in **Table 2**, the occult nodal metastasis rates are 30.9%, 23.8%, 15.1%, 12.7% and 12.9%, respectively. The ROC curves of all the above groups are displayed in **Fig. 3**. The NRI values of models compared with cN were visually displayed in **Fig. 4**, and all the *p* value were less than .001 except for RAD95 in both group all (*p*=.19) and group T1-2 (*p*=.04).

Discussion

Since the performance on evaluating neck metastasis by radiologists or existing assisted tool still remained unsatisfied, confusing the neck management of tongue cancer, in this study, we constructed and validated artificial neural network-based models with CT radiomics of primary tumors to predict neck lymph node metastasis in tongue cancer noninvasively and preoperatively, especially in the early stage group and occult metastatic lesions, with an improvement reaching

40% assessed with Net Reclassification Index (*p*<.001) and a reduction of occult node metastasis rate from 30.9% to a minimum of 12.7%.

Above all, the cohort in this study could be representative of the controversy regarding clinical neck management. Almost 80% of patients in this study suffered from T1-2 tumors, where occult nodal metastasis occurred most often,^{23,24} making it more difficult to detect the metastasis clinically, while ND was routinely performed in T3-4 cases. In addition, the occult nodal metastasis rate of T1-2 tumors in this study was 30.9%, close to a mean of 25.9%, ranging from 8.2-46.3%.²³

In this study, the primary tumor was chosen as the ROI. Recent proposed similar models originated from the features of either the primary tumor^{10,11} or the nodes.⁷⁻⁹ The former initially determines the node status by characteristics such as tumor budding, thickness and invasive depth,²⁵⁻²⁷ which could be better references for whether to perform ND and more feasible because the latter ignores the radiologically invisible nodes and is unable to make one-to-one matches from radiological nodes to pathological ones. Moreover, the decision is made prior to how to perform the ND as a result of the relatively distinct clinical characteristics of patients needing to undergo comprehensive ND and confusion between those of observation and selective ND under the guidance of the NCCN.

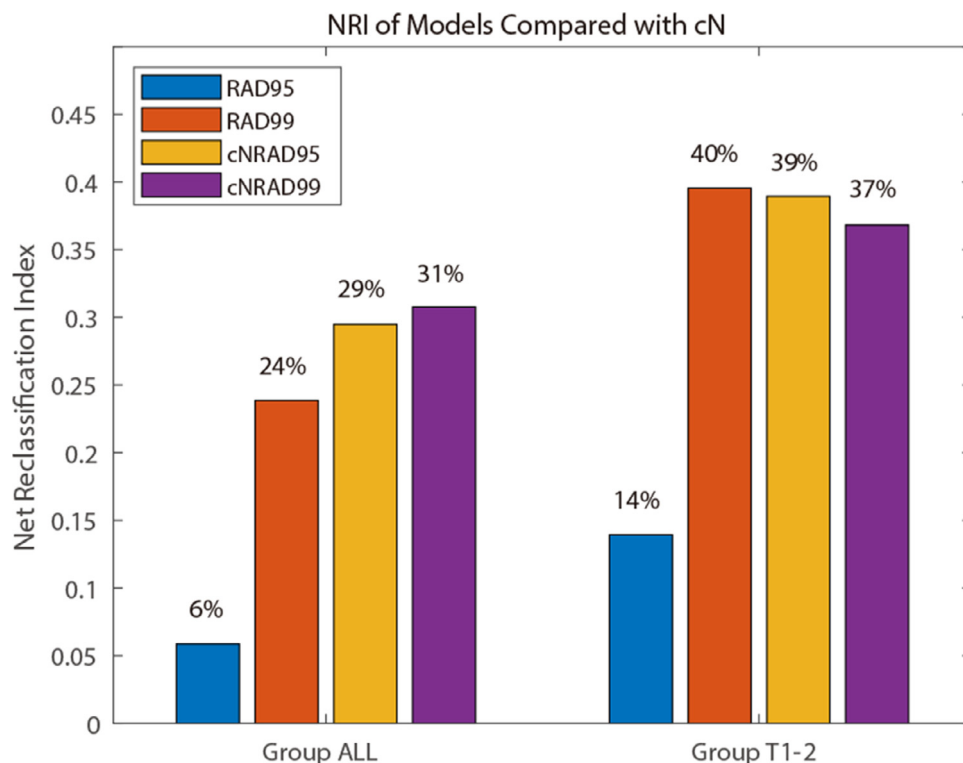


Fig. 4. The NRI values of models compared with cN in group All and group T1-2. All the models exceeded the naked eye evaluation, especially in group T1-2, with improvements up to 40%.

Encouragingly, the performance of these models was remarkable. Not only did the RAD99, cNRAD95 and nNRAD99 models outperformed the radiologists in this study in terms of the ACC and NRI or other reports^{4,5} in terms of both the SEN and SPE, but also showed a similar satisfying overall performance, such as with the ACC of the test set in a larger and more homogeneous dataset, and with more reliable and reproducible processes, such as semiautomatic segmentation, and more common CT machines, compared to the models from a study based on dual-energy CT texture with ACC, SEN and SPE values of 88%, 100% and 67%, respectively.¹⁰

Furthermore, our models show good discriminatory ability in cNO patients with AUCs ranging from 0.816 (95%CI:0.754–0.878, $p < .001$) to 0.913 (95%CI:0.754–0.878, $p < .001$) and ACCs ranging from 77.7% to 87.7%, especially in T1–2 tumors with AUCs ranging from 0.837 (95%CI:0.773–0.902, $p < .001$) to 0.933 (95%CI:0.899–0.967, $p < .001$) and ACCs ranging from 79.8% to 86.7%. It is widely known that the management of clinical negative LNs in patients with tongue cancer remains controversial globally^{28,29} due to the high occult nodal metastasis rate mentioned above. Even one node metastasis will decrease the survival rate by almost 50%.^{30,31} Work such as the construction of a series of patient-level machine learning models based on preoperative factors, such as age, sex, tobacco use and alcohol use, to predict early-stage tongue cancer neck metastasis have been done,¹¹ while the best-performing model (i.e., the RF model with an AUC of 0.786, a SEN of 0.85, and an SPE of 0.75) was inferior to most of our models based on CT scans. Besides, one of our models, cNRAD95, reduced the occult nodal metastasis rate from 30.9% to 12.7%, and the NRI showed 40% improvement from naked eyes evaluation in the T1–2 group ($p < .001$).

With the merits above, application based on our models during the clinical process might be expected, due to the relatively objective combined predictive information from tumor adding to neck evaluation. While for the time being, most clinicians and radiologists assess nodal status through palpable or radiologically visible nodes. Moreover, factors from primary tumors that affect the neck metastatic rate and mentioned above,^{25–27} are complex and often ignored for neck evaluation in the clinical process, and were potentially embedded in our models, which is more convenient, economics, non-invasive and equally accurate while compared with well-known precise method, positron emission tomography (PET) and node biopsy.^{4,5} Comprehensive information would be obtained and the clinical application for these models is promising. In addition, with the assistance of artificial neural network, tumor radiomics signatures may expand the connotation of T classification.

There were still limitations in this study. More steps could have been taken to improve the robustness of the features, such as imaging at multiple time points or combining multiple modeling methodologies.¹³ If possible, prospective work should be done to further validate the accuracy of the model.

Conclusions

In conclusion, we constructed and validated reliable ANN-based models that incorporated CT radiomics of primary tumors with traditional LN evaluations to more precisely predict cervical LN metastasis in patients with tongue cancer, especially in those with early-stage disease.

Declarations of interest

We have no Conflict of Interest.

Acknowledgements

This work was supported by the Program for New Clinical Techniques and Therapies of Peking University School and Hospital of

Stomatology (PKUSSNCT-19A07) and the Project of Clinical Key Department Construction of Peking University School and Hospital of Stomatology.

Supplementary materials

Supplementary material associated with this article can be found, in the online version, at doi:10.1016/j.neurad.2021.07.006.

References

- Cerezo L, Millan I, Torre A, Aragon G, Otero J. Prognostic factors for survival and tumor control in cervical lymph node metastases from head and neck cancer. A multivariate study of 492 cases. *Cancer*. 1992;69:1224–1234.
- Shingaki S, Takada M, Sasai K, et al. Impact of lymph node metastasis on the pattern of failure and survival in oral carcinomas. *Am J Surg*. 2003;185:278–284.
- Sano D, Myers JN. Metastasis of squamous cell carcinoma of the oral tongue. *Cancer Metastasis Rev*. 2007;26:645–662.
- Stokkel MP, ten Broek FW, Hordijk GJ, Koole R, van Rijk PP. Preoperative evaluation of patients with primary head and neck cancer using dual-head 18fluorodeoxyglucose positron emission tomography. *Ann Surg*. 2000;231:229–234.
- de Bondt RB, Nelemans PJ, Hofman PA, et al. Detection of lymph node metastases in head and neck cancer: A meta-analysis comparing US, USgFNAC, CT and MR imaging. *Eur J Radiol*. 2007;64:266–272.
- Sun J, Li B, Li CJ, et al. Computed tomography versus magnetic resonance imaging for diagnosing cervical lymph node metastasis of head and neck cancer: A systematic review and meta-analysis. *Oncol Targets Ther*. 2015;8:1291–1313.
- Kann BH, Aneja S, Loganadane GV, et al. Pretreatment identification of head and neck cancer nodal metastasis and extranodal extension using deep learning neural networks. *Scientific reports*. 2018;8:14036.
- Chen L, Zhou Z, Sher D, et al. Combining many-objective radiomics and 3D convolutional neural network through evidential reasoning to predict lymph node metastasis in head and neck cancer. *Phys Med Biol*. 2019;64. 075011.
- Ho TY, Chao CH, Chin SC, Ng SH, Kang CJ, Tsang NM. Classifying neck lymph nodes of head and neck squamous cell carcinoma in MRI images with radiomic features. *J Digital Imag*. 2020;33:613–618.
- Forghani R, Chatterjee A, Reinhold C, et al. Head and neck squamous cell carcinoma: prediction of cervical lymph node metastasis by dual-energy CT texture analysis with machine learning. *Eur Radiol*. 2019;29:6172–6181.
- Shan J, Jiang R, Chen X, et al. Machine learning predicts lymph node metastasis in early-stage oral tongue squamous cell carcinoma. *J Oral Maxillofac Surg*. 2020.
- Lambin P, Rios-Velazquez E, Leijenaar R, et al. Radiomics: Extracting more information from medical images using advanced feature analysis. *Eur J Cancer*. 2012;48:441–446.
- Lambin P, Leijenaar RTH, Deist TM, et al. Radiomics: The bridge between medical imaging and personalized medicine. *Nat Rev Clin Oncol*. 2017;14:749–762.
- Attye A, Ognard J, Rousseau F, Ben Salem D. Artificial neuroradiology: Between human and artificial networks of neurons? *J Neuroradiol*. 2019;46:279–280.
- Wu S, Zheng J, Li Y, et al. A radiomics nomogram for the preoperative prediction of lymph node metastasis in bladder cancer. *Clin Cancer Res*. 2017;23:6904–6911.
- Wang T, Gao T, Yang J, et al. Preoperative prediction of pelvic lymph nodes metastasis in early-stage cervical cancer using radiomics nomogram developed based on T2-weighted MRI and diffusion-weighted imaging. *Eur J Radiol*. 2019;114:128–135.
- Tan X, Ma Z, Yan L, Ye W, Liu Z, Liang C. Radiomics nomogram outperforms size criteria in discriminating lymph node metastasis in resectable esophageal squamous cell carcinoma. *Eur Radiol*. 2019;29:392–400.
- Huang YQ, Liang CH, He L, et al. Development and validation of a radiomics nomogram for preoperative prediction of lymph node metastasis in colorectal cancer. *J Clin Oncol*. 2016;34:2157–2164.
- Bourquin J, Schmidli H, van Hoogevest P, Leuenberger H. Advantages of Artificial Neural Networks (ANNs) as alternative modelling technique for data sets showing non-linear relationships using data from a galenic study on a solid dosage form. *Eur J Pharm Sci*. 1998;7:5–16.
- Zhu L, Kolesov L, Gao Y, Kikinis R, Tannenbaum A. An effective interactive medical image segmentation method using fast GrowCut. *International Conference on Medical Image Computing and Computer Assisted Intervention (MICCAI), Interactive Medical Image Computing Workshop*. 2014.
- Zhang L, Fried DV, Fave XJ, Hunter LA, Yang J, Court LE. IBEX: An open infrastructure software platform to facilitate collaborative work in radiomics. *Med Phys*. 2015;42:1341–1353.
- Pencina MJ, D'Agostino Sr. RB, D'Agostino Jr. RB, Vasan RS. Evaluating the added predictive ability of a new marker: from area under the ROC curve to reclassification and beyond. *Stat Med*. 2008;27:157–172. discussion 207–112.
- Abu-Ghanem S, Yehuda M, Carmel NN, et al. Elective neck dissection vs observation in early-stage squamous cell carcinoma of the oral tongue with no clinically apparent lymph node metastasis in the neck: a systematic review and meta-analysis. *JAMA Otolaryngol Head Neck Surg*. 2016;142:857–865.
- Lee JG, Litton WB. Occult regional metastasis: Carcinoma of the oral tongue. *Laryngoscope*. 1972;82:1273–1281.
- Mucke T, Kanatas A, Ritschl LM, et al. Tumor thickness and risk of lymph node metastasis in patients with squamous cell carcinoma of the tongue. *Oral Oncol*. 2016;53:80–84.

26. Mitani S, Tomioka T, Hayashi R, Ugumori T, Hato N, Fujii S. Anatomic invasive depth predicts delayed cervical lymph node metastasis of tongue squamous cell carcinoma. *Am J Surg Pathol.* 2016;40:934–942.
27. Matos LL, Manfro G, Santos RV, et al. Tumor thickness as a predictive factor of lymph node metastasis and disease recurrence in T1N0 and T2N0 squamous cell carcinoma of the oral tongue. *Oral Surg Oral Med Oral Pathol Oral Radiol.* 2014;118:209–217.
28. Yuen AP, Wei WI, Wong YM, Tang KC. Elective neck dissection versus observation in the treatment of early oral tongue carcinoma. *Head Neck.* 1997;19:583–588.
29. Huang SF, Kang CJ, Lin CY, et al. Neck treatment of patients with early stage oral tongue cancer: comparison between observation, supraomohyoid dissection, and extended dissection. *Cancer.* 2008;112:1066–1075.
30. Agarwal SK, Arora SK, Kumar G, Sarin D. Isolated perifacial lymph node metastasis in oral squamous cell carcinoma with clinically node-negative neck. *Laryngoscope.* 2016;126:2252–2256.
31. Shah JP. Patterns of cervical lymph node metastasis from squamous carcinomas of the upper aerodigestive tract. *Am J Surg.* 1990;160:405–409.